Compensation of Random and Systematic Timing Errors in Sampling Oscilloscopes

Paul D. Hale, *Senior Member, IEEE*, C. M. Wang, Dylan F. Williams, *Fellow, IEEE*,
Kate A. Remley, *Senior Member, IEEE*, and Joshua D. Wepman

***Abstract*—In this paper, a method of correcting both random and systematic timebase errors using measurements of only two quadrature sinusoids made simultaneously with a waveform of interest is described. The authors estimate the fundamental limits to the procedure due to additive noise and sampler jitter and demonstrate the procedure with some actual measurements.**

***Index Terms*—Comb generator, jitter, sampling oscilloscope, timebase distortion (TBD), waveform metrology.**

I. Introduction

HIGH-SPEED sampling oscilloscopes suffer from systematic timebase distortion (TBD) and random jitter that cause errors in the time at which samples of a signal are acquired. We propose an alternative timebase, for use with equivalent-time sampling oscilloscopes, that greatly reduces both TBD and jitter, assuming that the sampling times on the oscilloscope channels are sufficiently synchronized with one another, that is, assuming that the jitter of all the channels is sufficiently correlated. The new timebase relies on simultaneous measurement of the signal of interest and two reference sinusoids that are in quadrature and phase locked to the signal of interest that serve to determine the actual time at which the measurement was performed [1]. The conventional timebase of the oscilloscope is used to characterize distortion in the two reference sinusoids and to determine within which half-cycle of the auxiliary sinusoids the signal was measured. The new timebase is estimated from the sinusoids using a weighted "error-in-variables" approach that accounts for relative contributions of additive noise and timing error.

Sampling oscilloscopes that have a form of jitter correction based on quadrature sinusoidal reference signals are described elsewhere in the literature [2], and sampling oscilloscopes with similar functionality have recently become commercially available.[1,2] Our implementation achieves the advantages of these systems, including a residual jitter of about 200 fs, correction of time records with nearly arbitrary length, and application to measurement of signals at almost any frequency. Furthermore, our method is inexpensive since it can be implemented with an older generation of standard equipment. Our method corrects for *both* random jitter and systematic TBD and provides the user with an estimate of the residual timing error after the correction process has been applied. Also, our technique is nonproprietary and is described and characterized here, for the first time, in the open archival literature.

In an oscilloscope, the timing error at the ith sample, i.e., y_i, is the sum of the systematic TBD h_i, and random timing jitter error τ_i. Thus, the ith sample of the signal of interest g as a function of time is given by

$$y_i = g(T_i + h_i + \tau_i) + \varepsilon_i \tag{1}$$

where $T_i = (i-1)T_\mathrm{s}$ is the target time of each sample, T_s is the target time interval between samples, and ε_i is the additive noise. We assume that the jitter and additive noise are independent zero-mean random variables with variances σ_τ^2 and σ_ε^2.

The problem of estimating jitter and correcting for its effects has been addressed by many authors [3]–[7]. The typical approach is to obtain the signal variance of independent repeated measurements and use the approximate model [8], i.e.,

$$\mathrm{var}(y_i) \approx \sigma_\tau^2 \left(g'(t_i)\right)^2 + \sigma_\varepsilon^2 \tag{2}$$

to solve for σ_τ^2. Here, $g'(t_i)$ is the derivative of $g(t_i)$ evaluated at $t_i = T_i + h_i$. It is usually assumed that, upon averaging, the jitter acts as a lowpass filter, so that the average signal is the convolution of the signal $g(t_i)$ and the probability density function $p(\cdot)$ of the jitter, i.e.,

$$\langle g(t_i)\rangle = \int g(t_i - \tau)p(\tau)d\tau. \tag{3}$$

The effects of jitter are then removed by deconvolution [3].

Manuscript received October 18, 2004; revised May 8, 2006.

P. D. Hale is with the Optoelectronics Division, National Institute of Standards and Technology, Boulder, CO 80305 USA (e-mail: hale@boulder.nist.gov).

C. M. Wang is with the Statistical Engineering Division, National Institute of Standards and Technology, Boulder, CO 80305 USA.

D. F. Williams, K. A. Remley, and J. D. Wepman are with the Electromagnetics Division, National Institute of Standards and Technology, Boulder, CO 80305 USA.

Digital Object Identifier 10.1109/TIM.2006.880270

[1]Agilent 86107A precision timebase reference module. NIST does not endorse or guarantee this product. This product is listed here only to reference similar measurement techniques. Other products may perform as well or better than those listed here.

[2]Tektronix 82A04 phase reference module. NIST does not endorse or guarantee this product. This product is listed here only to reference similar measurement techniques. Other products may perform as well or better than those listed here.

This approach has the following problems.

1) Measurements must be repeated to find the measurement mean and variance.
2) Estimates of the jitter variance from (2) are generally biased (for example, see [7]).
3) $p(\cdot)$ must be known.
4) $p(\cdot)$ must be the same over the entire measured waveform.
5) The averaging process removes some of the inherent bandwidth from the measured signal, making the deconvolution subjective [9], [10].
6) Deconvolution is an "ill-posed" problem [10], so that in the presence of noise, there is no unique solution.

Generally, it is desirable to avoid deconvolution, particularly in cases where the jitter is large, varies over the measurement time window, or has a non-Gaussian probability density. All these situations make deconvolving the jitter from (3) problematic.

The problem of estimating TBD has also been studied by many authors [11]–[18]. Recent work [15]–[18] has used a nonlinear least squares approach that fits multiple measured sinusoids with multiple phases and frequencies to a distorted sinusoid model. This approach performs well at discontinuities in the TBD and allows simultaneous estimation of the harmonic distortion, if any, in the measured sinusoids. The distorted sinusoid model, with harmonic number n_h, is given by [16]

$$y_{ij} = \alpha_j + \sum_{k=1}^{n_h} \left[\beta_{jk}\cos(2\pi k f_j t_{ij}) + \gamma_{jk}\sin(2\pi k f_j t_{ij})\right] + \varepsilon_{ij} \tag{4}$$

where f_j is the fundamental frequency of the jth measured waveform y_{ij} at the ith nominal time, i.e., $t_{ij} = T_i + h_i + \tau_{ij}$. The random jitter is τ_{ij}, and ε_{ij} is the random additive noise. The values of α_j, β_{jk}, γ_{jk}, and h_i can be estimated by use of a weighted least squares approach [16]. To obtain a solution using this approach, we typically measure a set of sinusoidal waveforms at two or three different frequencies. Each set includes two sinusoids, of a given frequency, that are approximately in quadrature. Hence, each set can have up to four or six waveforms for which ε_{ij} and τ_{ij} are different for all i and j. When estimating TBD, we generally average over several measurement sets to average over different realizations of ε_{ij} and τ_{ij} and reduce the uncertainty due to random jitter and additive noise. Averaging over several measured waveforms is also required in the methods described in [16] and [17].

In this paper, however, we are interested in the total timebase error, i.e., the sum of the TBD and the jitter in an "individual realization" of a measured waveform. We use all of the information in the sinusoid to find the distortion (that is, we estimate α_j, β_{jk}, and γ_{jk}) and the timebase (h_i and τ_{ij}) simultaneously, so that the measured dependent variable (y_{ij}) best corresponds to the values of the distorted reference sinusoids with the new timebase. In this case, no averaging is involved.

A simple illustration is shown in Fig. 1, which plots uncorrected measurements (circles) of a reference sinusoid with an estimate of the distorted sinusoid (solid curve). Each circle represents a sample at time $t_i = T_i + h_i + \tau_i$, with each τ_i as a realization of a random process. The estimated sinusoid is found by minimizing the average "distance" between the samples and the sinusoid. If we assume, for illustrative purposes, that there is no additive noise, we can estimate the total time error due to TBD and jitter by drawing a horizontal line between each measurement (circles) and the distorted sinusoid. The length of each line represents the difference between the nominal (oscilloscope) time at which the measurement was taken and the time as determined by the distorted sinusoidal fit. The time that each line intersects the distorted sinusoid is the corrected time for each sample. Once the timebase error is known for each t_i, it can be applied to a simultaneously measured signal of interest *if* the timing errors of the simultaneous measurements are sufficiently correlated. In the next section, we discuss how this correlation is achieved.

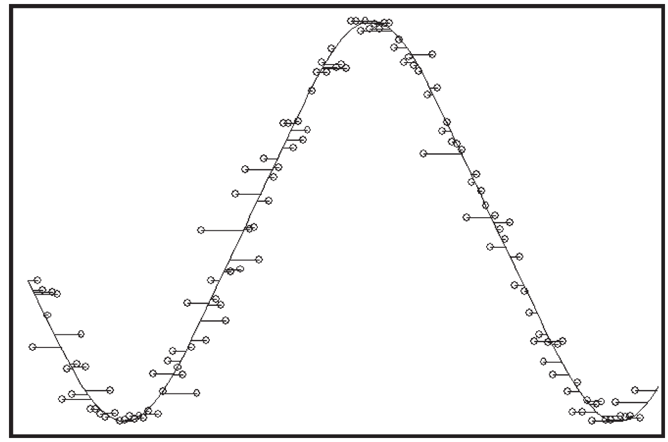

Fig. 1. Circles show sampled signal using distorted and jittered oscilloscope timebase, and the solid curve shows the estimated distorted sinusoid. Horizontal lines show difference between the time estimated from the curve and the nominal oscilloscope timebase.

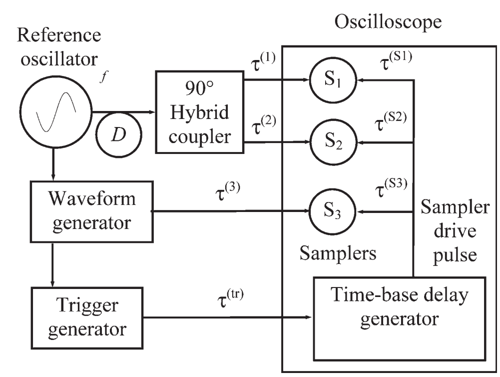

Fig. 2. Schematic diagram of generic system used to measure and correct oscilloscope timebase errors. The reference generator, waveform generator, and trigger generator are synchronized. Various sources of jitter are labeled as $\tau^{(\cdot)}$.

II. System for Measuring and Correcting Timebase Errors

Fig. 2 shows a generalized schematic of the signal generator and sampling system for correcting timebase errors. The reference oscillator generates a sinusoid with frequency f. The waveform generator and trigger generator are synchronized to the reference oscillator. We adjust the delay D, so that the signal propagation delay between the signal generator and samplers

1 and 2 is roughly the same as the delay between the signal generator and sampler 3. This is done to ensure minimal impact of the signal generator phase noise and maximal correlation between the reference sine waves and the waveform generator.

We take advantage of the parallel design of many equivalent-time sampling oscilloscopes. In such an oscilloscope, the sampling process proceeds as follows [13], [19]: 1) The timebase is armed to trigger on a rising or falling edge at a certain level; 2) a pulse with the desired characteristics is sent into the trigger input, triggering the timebase; 3) the timebase (delay generator) waits for a predefined time delay; and then, 4) the timebase generates a drive (strobe) pulse that is split and sent simultaneously to *all* the samplers in the oscilloscope mainframe. A waveform is sampled by incrementing the time delay by a nominal increment $T_{\rm s}$ and repeating the process. A result of the parallel architecture is that any jitter on the trigger pulse or the timebase delay generator is common to the sampling time of all the samplers in the oscilloscope mainframe.

In Fig. 2, we show the sources of jitter, measured relative to an absolute reference oscillator. They include $\tau^{(1)}$ and $\tau^{(2)}$, which are the jitter of the reference signals. We expect that these have the same statistical properties (mean 0 and standard deviation $\sigma^{(1)} \simeq \sigma^{(2)}$), although their individual realizations for the ith sample might differ slightly. The value of $\tau^{(3)}$ is the jitter of the generated waveform we want to measure and has mean 0 and standard deviation $\sigma^{(3)}$. The value of $\tau^{(\rm tr)}$ is the jitter of the trigger generator and timebase generator circuit and has mean 0 and standard deviation $\sigma^{(\rm tr)}$. We also include a jitter $\tau^{(Sx)}$ $(x = 1, 2, 3)$ for the actual sampling process for each of the samplers, with mean 0 and standard deviation $\sigma^{(S1)} \simeq \sigma^{(S2)} \simeq \sigma^{(S3)}$.

When the samplers are simultaneously fired from the same trigger event, the different jitter components contribute to the sampled signals as follows:

$$\begin{aligned} S_1(t_i) &= S_1\left(T_i + h_i + \tau_i^{(1)} + \tau_i^{(S1)} + \tau_i^{(\rm tr)}\right) \\ S_2(t_i) &= S_2\left(T_i + h_i + \tau_i^{(2)} + \tau_i^{(S2)} + \tau_i^{(\rm tr)}\right) \\ S_3(t_i) &= S_3\left(T_i + h_i + \tau_i^{(3)} + \tau_i^{(S3)} + \tau_i^{(\rm tr)}\right). \end{aligned} \tag{5}$$

We note that h_i and $\tau_i^{(\rm tr)}$ are common to all the simultaneously strobed samples. Hence, if $\sigma^{(\rm tr)} \gg \sigma^{(x)}$ and $\sigma^{(\rm tr)} \gg \sigma^{(Sx)}$ $(x = 1, 2, 3)$, $\tau_i^{(\rm tr)}$ is the dominant source of jitter, and we can approximate τ_{ij} as $\tau_i^{(\rm tr)}$. Furthermore, if we can estimate h_i and realizations of $\tau_i^{(\rm tr)}$ from the known sinusoidal signals $S_1(t_i)$ and $S_2(t_i)$, we can apply our estimate to the third waveform, i.e., $S_3(t_i)$, and compensate for timing errors in its measurement.

III. Estimating Random Jitter

Our approach to estimating the timing errors in (4) is to apply the so-called errors-in-variables [20] or orthogonal distance regression (ODR) [21] to the model in (4). In this approach, the distorted sinusoid model is fit to the data with the assumption that both "dependent" (y_i) and "independent" (t_{ij}) variables are subject to errors. Specifically, let y_{i1} and y_{i2} be the ith samples of nearly quadrature sinusoids measured simultaneously with the signal of interest. Denote the total timing error as $\delta_{ij} = h_i + \tau_{ij}$, $j = 1, 2$. Then, δ_{i1} and δ_{i2} are the timing errors of the two sinusoid measurements. Because the samplers are driven by a common strobe pulse, as described in the previous section, we assume equal timing errors in channels 1 and 2. That is, we assume $\tau_{i1} = \tau_{i2} = \tau_i$, and hence, $\delta_i = \delta_{ij} = h_i + \tau_i$ and $t_i = t_{ij} = T_i + \delta_i$. We rewrite y_{ij}, given in (4), as a function F of $\boldsymbol{\theta}_j = (\alpha_j, \beta_{j1} \ldots \beta_{jn_h}, \gamma_{j1} \ldots \gamma_{jn_h})$ as

$$y_{ij} = F(T_i + \delta_i; \boldsymbol{\theta}_j) + \varepsilon_{ij}.$$

Estimates of timing errors δ_i are readily available from the ODR fit of the model using ODRPACK [21]. Although other numerical packages may also work for this application, ODRPACK has been extensively tested, shown to work well, and is freely available [22]. The ODR procedure obtains the best fit model for this problem by minimizing the error function

$$\begin{aligned} E(\boldsymbol{\theta}_1, \boldsymbol{\theta}_2, \boldsymbol{\delta}) &= \sum_{i=1}^{n} \left\{ \frac{w_\varepsilon}{2}\left(\varepsilon_{i1}^2 + \varepsilon_{i2}^2\right) + w_\delta \delta_i^2 \right\} \\ &= \sum_{i=1}^{n} \left\{ \frac{w_\varepsilon}{2}\Big([F(T_i + \delta_i; \boldsymbol{\theta}_1) - y_{i1}]^2 \right. \\ &\qquad \left. + [F(T_i + \delta_i; \boldsymbol{\theta}_2) - y_{i2}]^2 \Big) + w_\delta \delta_i^2 \right\} \end{aligned} \tag{6}$$

with respect to $\boldsymbol{\theta}_1$, $\boldsymbol{\theta}_2$, and $\boldsymbol{\delta} = (\delta_1, \ldots, \delta_n)$ (n is the number of points in each waveform).

The weights w_ε and w_δ are inversely proportional to the variances σ_ε^2 and σ_δ^2. That is, $w_\varepsilon = 1/\sigma_\varepsilon^2$ and $w_\delta = 1/\sigma_\delta^2$. If the TBD is small relative to σ_τ or if an adequate TBD estimate is available as an initial guess of the timebase error δ_i, then $\sigma_\delta^2 \approx \sigma_\tau^2$ and $w_\delta = 1/\sigma_\tau^2$. Equivalently, we can use $w_\varepsilon = \sigma_\tau^2/\sigma_\varepsilon^2$ and $w_\delta = 1$ in (6). We note that with these weights and the assumptions that ε_{ij} $(j = 1, 2)$ and δ_i are normally distributed with mean 0 and known variances σ_ε^2 and σ_τ^2, the least squares estimators of $\boldsymbol{\theta}_1$, $\boldsymbol{\theta}_2$, and $\boldsymbol{\delta}$ are also maximum likelihood estimators. Further discussions on the use of the weights are given in the Appendix.

IV. Practical Considerations

This ODR approach works well for most of the data we observe in our laboratory and requires only two nearly quadrature sinusoids. There are instances, however, where the ODR approach produces unsatisfactory results. This is the case when the waveform is very long, there are only a few samples per cycle of the sinusoid, or when the TBD is large (compared with the jitter). In such cases, we use an estimate of the TBD as an initial guess for the total timebase error to help the ODR routine converge to a solution. This initial TBD estimate requires additional measurements of quadrature sinusoids at different frequencies. These additional measurements need not be made simultaneously with the signal of interest. Criteria for frequency selection for the TBD estimate are described in detail in [15].

Additive noise on the reference sinusoids can be a source of error in any timebase error correction. From (2), we see that the frequency f of the sinusoid $g(t)$ should be chosen such that $\sigma_\tau^2(g'(t))^2 > \sigma_\varepsilon^2$ over most of the sinusoid. That is, to achieve good discrimination between jitter and additive noise, the slew rate must be high enough, so that the jitter becomes the dominant noise process for most of the sinusoid. For our sinusoid, we require $\sigma_\tau^2(2\pi f A)^2 > \sigma_\varepsilon^2$, or $2\pi f \sigma_\tau > \sigma_\varepsilon / A$, where A is the amplitude of the sine wave. We will discuss this bound further in the next section.

From the above discussion, we conclude that we want f as large as possible. However, since we need to discriminate between half-cycles of the reference sine waves, we also require that $\sigma_\tau \ll 1/(2f)$ to make the probability of shifting a point to the wrong quarter cycle acceptably small. Combining these limits and rearranging gives us practical bounds for selecting the frequency of the reference sinusoid: $1/2 \gg f\sigma_\tau > \sigma_\varepsilon/(2\pi A)$.

We can estimate an upper bound for the root-mean-square (rms) residual timing error (after correction) e_Δ due to additive noise, in the limit of zero jitter, as $e_\Delta = \sigma_\varepsilon/(2\pi f A)$. For a 10-GHz sinusoid and $(\sigma_\varepsilon/A) = 0.1\%$, 1%, and 5%, we obtain $e_\Delta = 0.016, 0.16,$ and 0.8 ps, respectively.

V. Simulation Studies

We used simulation to investigate the proposed method for estimating the timing error and to verify the fundamental limits imposed by additive noise suggested in the previous section. The criterion used in the comparisons is the amount of timing error remaining in a waveform of interest after both random and systematic timebase errors were corrected using the estimation procedure.

Recall from (1) that the actual time of the ith sample is given by

$$t_i = T_i + h_i + \tau_i.$$

With estimates (denoted by $\hat{}$) of the TBD $\hat{h}_i$ and the realization of the jitter $\hat{\tau}_i$, obtained by the estimation procedure, our estimate of t_i is then given by

$$\hat{t}_i = T_i + \hat{h}_i + \hat{\tau}_i.$$

The remaining timing errors can be characterized by the sample standard deviation s_Δ of

$$\Delta_i = t_i - \hat{t}_i = h_i + \tau_i - (\hat{h}_i + \hat{\tau}_i) \qquad (7)$$

where h_i and τ_i are the simulated TBD and jitter used in the simulation.

We generated sinusoids according to (4) to simulate actual measurements. The simulation parameters used here, including TBD, are closely related to those we observe in our laboratory. We used a time-measurement window (waveform epoch) of 52 ns with 53 248 samples. Since the TBD would be large for this long time record, we estimated the TBD (using the method of [16]) and used it as an initial guess for the total time error. We generated 100 sets of six sinusoids, including pairs of 0° and 90° phases at three different frequencies. In addition to estimating the timebase error, we also use the 10-GHz 0° sinusoid as the signal of interest, as described in the next paragraph. Each pair had equal timing error but uncorrelated additive noise. The signal frequencies and amplitudes are given in Table I, along with the amplitude of the harmonics ($n_h = 3$). In each simulation experiment, the additive noise was generated using a normal distribution with mean 0 and standard deviation σ_ε. The random jitter was generated using a normal distribution with mean 0 and standard deviation σ_τ. We also saved the nominal realization of the random jitter for the purpose of calculating Δ_i and s_Δ.

TABLE I
Amplitude of Fundamental and Harmonics Used in the Simulation Study

Fundamental frequency, GHz	Harmonic amplitude, V		
	Fundamental	Second harmonic	Third harmonic
10.0000	0.150	0.0006	0.007
9.8855	0.150	0.0006	0.007
10.2855	0.150	0.0002	0.0003

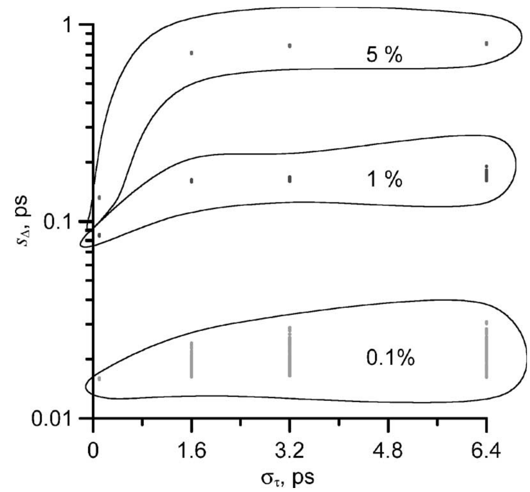

Fig. 3. Sample standard deviation for all 100 simulated data sets for each of 12 different combinations of σ_ε and σ_τ. Individual symbols are not resolved in this figure.

Fig. 3 shows s_Δ from each of the 100 simulations of the 10-GHz 0° sinusoids for each combination of $\sigma_\varepsilon = 0.1\%$, 1.0%, and 5.0% of the fundamental amplitude and $\sigma_\tau = 0.1, 1.6, 3.2,$ and 6.4 ps used in the simulation experiments. Fig. 3 shows that our procedure is effective for correcting the timing errors even in the presence of additive noise. Using the proper weighting for low initial jitter allows us to achieve s_Δ that is comparable to or below the simple estimate e_Δ. In contrast, for the case of larger initial jitter, s_Δ was approximately bounded by e_Δ.

Discussion of some particular cases in Fig. 3 is useful. For the case of $\sigma_\tau = 0.1$ ps and $\sigma_\varepsilon = 5.0\%$ of the fundamental amplitude, we have $f\sigma_\tau = 0.001 < \sigma_\varepsilon/(2\pi A) = 0.008$, violating our practical guidelines from Section IV. In this case, our simulations show that $s_\Delta > \sigma_\tau$. For the case of $\sigma_\tau = 1.6$ ps and $\sigma_\varepsilon = 5.0\%$ of the fundamental amplitude, we have $f\sigma_\tau = 0.016$, which is about two times larger than $\sigma_\varepsilon/(2\pi A) = 0.008$. In this case, our simulations show s_Δ roughly a factor of 2

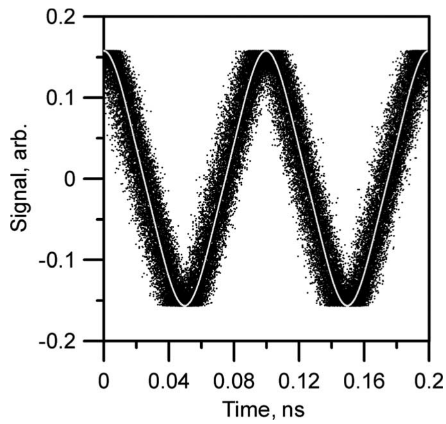

Fig. 4. Plot of one of the simulated 52-ns-long 10-GHz 0° sinusoids with (light dots) and without (black dots) correcting timing errors. See text for explanation.

smaller than σ_τ. Finally, in the case of very small initial additive noise, our simulations show the sample standard deviation s_Δ of the timing errors to be on the order of 0.02 ps. We will show in Section VI that we cannot achieve such low residual timing error because the jitter due to the samplers themselves becomes significant.

We plot one of the simulated 10-GHz 0° sinusoids with and without correcting the timing errors in Fig. 4. The long waveform (520 periods in our simulated experiments) is shown as a series of overlapping short waveforms (two periods in this example), which is similar to an eye pattern. The widely scattered points are the sinusoid generated with $\sigma_\tau = 3.2$ ps and $\sigma_\varepsilon = 1\%$ of the amplitude. The overlaying (lightly shaded) points are the sinusoid after correction for timebase errors. It can be seen from Fig. 4 that after correction, the errors have been collapsed to such a small level that they cannot be resolved on this scale.

We next consider the effects of using the incorrect harmonic order in the estimation procedure. In general, the harmonic distortion that is not accounted for will have the same effect as having an inflated additive noise, with the magnitude of the effect depending on the magnitude of the distortion that is not accounted for. As an example, we simulated a signal with $\sigma_\tau = 3.2$ ps, $\sigma_\varepsilon = 1\%$ of the fundamental amplitude, but $n_h = 5$, and with the amplitudes of the actual fourth and fifth harmonics equal to those of the second and third. If we use only three harmonic terms to correct the timing errors, the mean value of s_Δ (for 100 simulations) is about 1.167 ps, which is a substantial increase from 0.165 ps (given in Fig. 3). However, if harmonic distortion in the fourth and fifth is negligible, we do not see a substantial increase. For example, if the amplitudes of the fourth harmonic for all three frequencies are all 0.1 mV, and the amplitudes of the fifth harmonic of the three frequencies are 0.7, 0.7, and 0.1 mV, then the resulting mean value of s_Δ is only 0.196 ps. It is therefore necessary to have some knowledge of the number of harmonics n_h, which can be obtained using the method described in [16].

Weighted least squares procedures [15]–[17] can also be used in place of the ODR procedure to estimate the timebase error. We used 100 simulated data sets having $\sigma_\varepsilon = 0.1\%$ of the fundamental amplitude and $\sigma_\tau = 1.6$ ps to compare the performance of the weighted least squares and the ODR procedures. We first estimated the TBD based on the 100 measurement sets at all the three frequencies. If we used this TBD estimate as the final timebase error without further adjustments, the mean of the 100 s_Δ was found to be 1.598 ps, which, as expected, is in agreement with the initial jitter standard deviation of 1.6 ps. We then used this TBD estimate as the initial timebase error and employed the weighted least squares [16] on each of the 100 10-GHz measurements to estimate the final timebase error. The weight used for y_i is the reciprocal of $\sigma_\varepsilon^2 + (g'(t_i))^2\sigma_\tau^2$. The mean of the 100 s_Δ was found to be 0.84 ps, which is substantially larger than the mean of the 100 s_Δ obtained using the ODR approach (see Fig. 3).

The difference in performance between the weighted least squares and the ODR approaches may lie in the implementation of the procedures. The algorithm implemented in the public-domain software package ODRPACK is an efficient and stable trust-region procedure [23]. It is more convenient to specify the model and incorporate the assumption of having common jitters between the two nearly quadrature sinusoids using the ODR approach. In addition, the package contains many error-checking facilities as well as an automatic scaling algorithm and has been extensively tested.

VI. Experimental Studies

In this section, we describe experiments that verify our compensation technique. These are example measurements where timebase correction is particularly important, including cases with large jitter or long time windows where TBD can give significant errors.

A. *Experimental Study 1: A Single Sinusoid*

We tested the assumption that the trigger and timebase generator are the dominant sources of jitter ($\sigma^{(\mathrm{tr})} \gg \sigma^{(Sx)}$), which is necessary for our method to be useful, by measuring an "unknown" sinusoid (on sampler 3 of Fig. 2) that was split from the 10-GHz reference signal generator using a 3-dB splitter. The other output of the splitter was further split in a hybrid coupler to provide 0° and 90° reference signals to samplers 1 and 2 of Fig. 2. The reference signals were provided by the clock output of a digital pattern generator, and the oscilloscope was triggered at 1/16 of the clock frequency using the trigger output of the pattern generator. After measuring 50 sets of these three sinusoids, we changed the reference frequency to the others listed in Table I and measured 50 sets of 0° and 90° sinusoids at those frequencies as well. Using the jitter estimation software in the oscilloscope, we estimated the jitter of the uncorrected measurement to have standard deviation of about 3.3 ps. From a separate measurement, with no input to samplers 1 and 2, we found that the rms additive noise was about 0.3% of the reference signal amplitude.

Because the sinusoid to be corrected and the reference signals are derived from the same source, we expect that the jitters $\tau_i^{(1)}$, $\tau_i^{(2)}$, and $\tau_i^{(3)}$ of the "unknown" sinusoid are highly correlated and, therefore, nearly equal. Hence, we

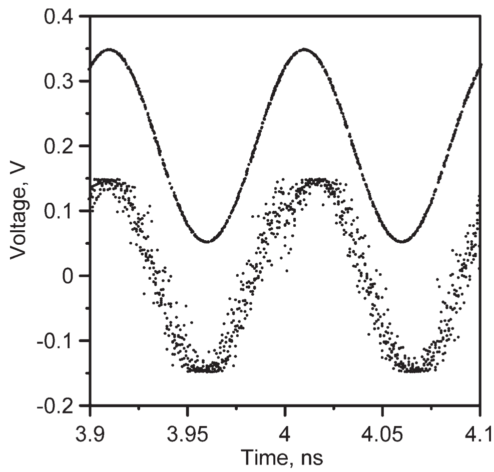

Fig. 5. Portion of five sinusoids measured on sampler 3 before (bottom) and after (top) correction for timebase errors. The offset between the curves has been added for clarity.

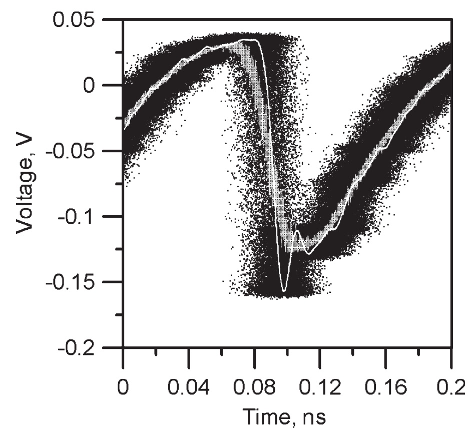

Fig. 6. Comparison of raw measurement (black dots), averaged measurement (noisy gray line), and timebase-corrected and averaged measurement (smooth light line).

expect this experiment to be insensitive to these parameters, with the remaining jitter being predominantly due to the jitter $\tau^{(Sx)}$ $(x = 1, 2, 3)$ in the samplers.

Because of the long time record used in this experiment, we estimate the TBD [16] as an initial guess for the ODR routine using $n_h = 3$ and all three measured frequencies. Fig. 5 shows a section of five of the 10-GHz sinusoids measured by the third sampler before (bottom) and after (top) correction for timebase errors. The uncorrected measurement has a discontinuity at 4 ns due to TBD, and the random noise is large where the slope is large, indicating significant jitter in the measurement. The corrected sinusoids have the discontinuity removed and exhibit noise that is greatly reduced and evenly distributed in time. Note that the waveforms shown in Fig. 5 have *not* been averaged.

We cannot use the procedure described in Section IV to evaluate the residual timing error because, for experimental data, both h_i and τ_i are unknown. If the waveforms of interest are known to be sinusoidal, as in this example, we can use the ODR procedure [21] to obtain an estimate of the residual timing error after correction. This is obtained from a sum of squares of the residuals of the ODR fit in the "independent" (t_{ij}) variable. The mean of the sample standard deviations of the residuals in $\hat{t}_i$ obtained from an ODR fit to 50 sinusoids measured in sampler 3 was found to be 0.2 ps. Thus, our experimental results show a jitter considerably larger than the numerical results of Fig. 3. From this, we conclude that the jitter $\tau^{(Sx)}$ of the samplers is not negligible but is still much smaller than the original jitter in the measurement. We estimated the jitter of one of the samplers using the estimated numerical limit of 0.021 ps, for our initial jitter and additive noise from Fig. 3, as $\sqrt{0.2^2 - 0.021^2}/\sqrt{2} = 0.14$ ps, where we have divided by $\sqrt{2}$ because the jitter is evenly distributed between sampler 3 and the sampler that is predominantly used as the reference signal for any given sample. This gives an estimated lower bound to our timebase correction due to sampler jitter: $0.14\sqrt{2} \approx 0.2$ ps. Although the sampler jitter is not negligible, it is 23 times smaller than the initial jitter in this experiment and about a factor of 6 smaller than the lowest jitter we observe in any of our laboratory measurements. We conclude that $\sigma^{(\mathrm{tr})}$ is sufficiently large compared with $\sigma^{(Sx)}$ and therefore expect reduced timebase error by using our procedure.

B. Experimental Study 2: Fast Transient With Jitter

In some measurement situations, such as those requiring averaging, (3) shows that jitter will blur details of a fast transient event, such as the output of a comb generator used for calibrating various high-speed measurement equipment. In the context of this paper, measurement of a fast transient allows us to use (2) to obtain an estimate of the residual jitter, after our correction, that is independent of the ODR algorithm. As stated before, jitter estimates made using (2) will have some bias but have sufficient accuracy for the present purposes.

To generate our fast transient, we used a 6-GHz signal generator to drive a nonlinear transmission line (NLTL). The NLTL was configured to steepen the falling edge of the generated sinusoid, giving a fast transient with a 6-GHz repetition rate. The output of the signal generator was split between a countdown trigger generator used to trigger the oscilloscope, the NLTL, and a hybrid coupler whose outputs were used as the reference signals on samplers 1 and 2. The measured transient from the NLTL (without deconvolution of the oscillscope impulse response) has roughly a 9-ps fall time.

By changing the trigger level of the oscilloscope, we can change the rms jitter from about 1.4 ps to more than 8.6 ps (as measured by the oscilloscope). Additive noise on the reference signals was about 0.4% of the sinusoid amplitude. Fig. 6 shows 50 measurements of the waveform generated by the NLTL before averaging (black dots) and after averaging (noisy gray line) for the case where the rms jitter is 8.6 ps. The light smooth curve in Fig. 6 is the result of the following correction and averaging procedure: 1) Each of the 50 waveforms was corrected for timebase errors; 2) each corrected waveform was linearly interpolated back to the original evenly spaced time grid; and 3) the resulting curves were averaged. This estimated waveform has much less noise but has ripple, ringing, and sharp features that are blurred in the corresponding average of the uncorrected measurements.

Fig. 7 shows an expanded view of the waveform after applying our procedure with three different initial values of

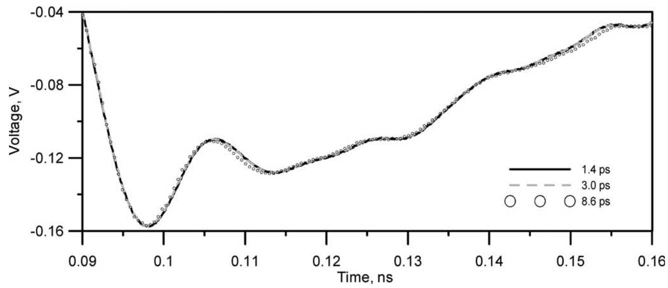

Fig. 7. Comparison of some corrected and averaged measurements. Measurements with initial jitter of 1.4 and 3.0 ps are indistinguishable on this scale, whereas the measurement with initial jitter of 8.6 ps shows differences as large as 1.4 ps at some times.

TABLE II
RESIDUAL JITTER ON MEASURED NLTL WAVEFORM

Initial rms jitter as measured on oscilloscope, ps	Residual rms jitter after correction, ($w = \sigma_\tau^2/\sigma_\varepsilon^2$), ps
1.4	0.15
3.0	0.20
6.3	0.25
8.6	0.25

jitter. Notice that the curves lie nearly on top of each other. Because the ringing and ripple are accurately represented in each reconstructed waveform, these features are *not* artifacts of the signal processing, as might be expected with some kinds of regularized noncausal deconvolution [9].

Closer inspection of the curves in Fig. 7 shows systematic time differences in the curves that increase with initial jitter but are still substantially less than the initial jitter. The two lowest jitter curves typically agree to within 100 fs, whereas the lowest and highest jitter cases differ by as much as 1.1 ps at some times. This systematic difference between the high and low jitter cases may be caused by the high noise level of the high jitter case, which leads to poor estimation of the harmonic content in the reference signal. It should be noted that 8.6 ps is on the order of three to ten times larger than the jitter we observe in typical measurements. Further investigation of this source of error is beyond the scope of this paper. The calculated fall times (10%–90% of peak-to-peak transition durations) of all four cases are indistinguishable.

Because we do not have an analytic expression for the fast transient, we cannot use the ODR approach to estimate the residual timing error in its measurement after correction. To estimate the residual jitter in the transient measurement, we used (2) on the corrected and linearly interpolated waveforms. Interpolation to a uniform grid allows us to estimate the variance and derivative at a given time, as is needed in (2). The results of our estimate are shown in Table II. We observe that the results for the experiments with most similar initial jitter (3.2 ps in sinusoidal experiment and 3.0 ps in NLTL experiment) are in good agreement; both have 0.2-ps residual jitter after correction and include the same amount of error from sampler jitter. Table II also shows that the resulting residual jitter is only weakly dependent on the initial jitter, as expected from the simulations in Section IV, and that the algorithm can improve a high jitter measurement by as much as 34 times (from 8.6 to 0.25 ps).

VII. DEMONSTRATION PROGRAM

Our program for postprocessing acquired waveforms for timebase correction has a graphical user interface that can be used in a Microsoft Windows[3] environment. The program, which is available at http://www.boulder.nist.gov/div815/HSM_Project/HSMP.htm, contains examples of how the software can be used to correct single or multiple measurements. These examples can be accessed through the program's help menu under "Getting Started." Instructions are also given on how to call the program from other programs with ActiveX[3] capability.

In addition to the TBD and jitter considered in this paper, our procedure also facilitates some limited correction for timebase drift. That is, if the initial time of a waveform drifts due to changes in trigger delay while making multiple measurements of a waveform, this change in delay is tracked by the phase of the reference sinusoids. Our software includes an option to subtract the delay, relative to the first acquired sinusoid. This procedure does not correct for drift in the measured waveform that is not correlated with drift in the reference sinusoids. Other procedures, such as those described in [7], [19], and [24], are required to correct for drift that is not correlated with the drift observed in the reference sinusoids.

VIII. CONCLUSION

We have shown how to simultaneously estimate the systematic and random timebase errors of measured sinusoidal reference signals. The parallel (simultaneous) sampling architecture of the oscilloscope allows us to use this estimate to correct the timebase errors in a simultaneously measured waveform by roughly a factor of 10, effectively replacing the timebase of the oscilloscope with a timebase provided by the measured sinusoids. We require only that the oscilloscope timebase have enough accuracy to allow us to discriminate between consecutive cycles of the reference signal and that there is sufficient correlation between the waveform of interest and the reference sinusoid. This allows us to correct the timing errors that might be present with long waveforms or large jitter and lowers the noise floor significantly in most measurements without averaging. In addition to the examples described in this paper, we have also demonstrated clear reduction of effects due to random jitter and TBD in measurements of 10-Gb/s data sequences that are 52 ns (53 248 samples) long and multisine signals that are 500 ns (40 960 samples) long.

APPENDIX

If σ_τ^2 and σ_ε^2 are not known or cannot be accurately estimated, the following procedure may be used to obtain an approximate estimate of the relative weight $\sigma_\tau^2/\sigma_\varepsilon^2$. The procedure is based

[3]NIST does not endorse or guarantee this product. This product is listed here only to provide the reader with information on how to use the software. Other products may perform in this application as well or better than those listed here.

on the assumption that an adequate TBD estimate is available as an initial guess of the timebase error.

The procedure first estimates the timing errors using $w_\varepsilon = w_0 = 1\ \mathrm{ns}^2/\mathrm{V}^2$. Let S_δ and S_ε be the weighted sums of squared residuals for δ and ε, respectively, from the ODR fit. If $S_\delta \approx S_\varepsilon$, then the correct weight has been used. Otherwise, use the new weight $w_\varepsilon = w_0 S_\delta / S_\varepsilon$ in the next ODR fit. Then, repeat this process until $S_\delta \approx S_\varepsilon$. For example, for the case where $\sigma_\varepsilon = 0.1\%$ of the fundamental and $\sigma_\tau = 6.4$ ps in the simulated experiment of Section V, using $w_\varepsilon = 1\ \mathrm{ns}^2/\mathrm{V}^2$ in the ODR fit produces $S_\delta = 2.124$ and $S_\varepsilon = 0.02572$ for the first set of measurements. (For illustration, we only report the results for the first set of measurements. Results for the other 99 sets of measurements are very similar.) A new weight of $w_\varepsilon = (2.124)/(0.02572) = 82.58$ in the next ODR fit produces $S_\delta = 2.173$ and $S_\varepsilon = 0.09923$. The next weight to use is $w_\varepsilon = (82.58\,\mathrm{ns}^2/\mathrm{V}^2)(2.173)/(0.09923) = 1808.388$, which produces $S_\delta = 2.174$ and $S_\varepsilon = 2.164$. The correct weight for this problem is 1820.4 $\mathrm{ns}^2/\mathrm{V}^2$. For the case where $\sigma_\varepsilon = 5\%$ of the fundamental and $\sigma_\tau = 3.2$ ps, one iteration yields a weight of 0.188 $\mathrm{ns}^2/\mathrm{V}^2$, which is close to the correct weight of 0.182 $\mathrm{ns}^2/\mathrm{V}^2$. For other combinations of σ_ε and σ_τ, it generally requires one or two iterations to obtain a "close" estimate of the correct relative weight.

ACKNOWLEDGMENT

The authors would like to thank M. Van Pelt for the loan of the NLTL; A. O'Gallagher for the help with generating the dynamic link libraries (DLLs) for the Visual Basic interface; and T. Clement, J. Scott, D. Larson, and the journal reviewers for their detailed review and useful comments that improved this paper.

REFERENCES

[1] S. H. Pepper, "Synchronous sampling and applications to analytic signal estimation," in *Proc. 56th ARFTG Conf. Dig.*, Dec. 2000, pp. 170–179.
[2] R. L. Jungerman, G. Lee, O. Buccafusca, Y. Kaneko, N. Itagaki, R. Shioda, A. Harada, Y. Nihei, and G. Sucha, "1-THz bandwidth C- and L-band optical sampling with a bit rate agile timebase," *IEEE Photon. Technol. Lett.*, vol. 14, no. 8, pp. 1148–1150, Aug. 2002.
[3] W. L. Gans, "The measurement and deconvolution of time jitter in equivalent-time waveform samplers," *IEEE Trans. Instrum. Meas.*, vol. IM-32, no. 1, pp. 126–133, Mar. 1983.
[4] J. Verspecht, "Compensation of timing jitter-induced distortion of sampled waveforms," *IEEE Trans. Instrum. Meas.*, vol. 43, no. 5, pp. 726–732, Oct. 1994.
[5] G. Vandersteen and R. Pintelon, "Maximum likelihood estimator for jitter noise models," *IEEE Trans. Instrum. Meas.*, vol. 49, no. 6, pp. 1282–1284, Dec. 2000.
[6] M. G. Cox, P. M. Harris, and D. A. Humphreys, "An algorithm for the removal of noise and jitter in signals and its application to picosecond electrical measurement," *Numer. Algorithms*, vol. 5, no. 1–4, pp. 491–508, Nov. 1993.
[7] K. J. Coakley, C. M. Wang, P. D. Hale, and T. S. Clement, "Adaptive characterization of jitter noise in sampled high-speed signals," *IEEE Trans. Instrum. Meas.*, vol. 52, no. 5, pp. 1537–1547, Oct. 2003.
[8] T. M. Souders, D. R. Flach, C. Hagwood, and G. L. Yang, "The effects of timing jitter in sampling systems," *IEEE Trans. Instrum. Meas.*, vol. 39, no. 1, pp. 80–85, Feb. 1990.
[9] N. S. Nahman and M. E. Guillaume, *Deconvolution of Time Domain Waveforms in the Presence of Noise*, Oct. 1981, Taipei, Taiwan, R.O.C.: National Bureau of Standards. NBS Technical Note 1047.
[10] A. N. Tikhonov and V. Y. Arsenin, *Solutions of Ill-Posed Problems*. Washington, DC: V. H. Winston and Sons, 1977.
[11] J. R. Scott, Jr., "Error corrections for an automated time-domain network analyzer," *IEEE Trans. Instrum. Meas.*, vol. IM-35, no. 3, pp. 300–303, Sep. 1986.
[12] J. Verspecht, "Accurate spectral estimation based on measurements with a distorted-timebase digitizer," *IEEE Trans. Instrum. Meas.*, vol. 43, no. 2, pp. 210–215, Apr. 1994.
[13] J. B. Retting and L. Dobos, "Picosecond time interval measurements," *IEEE Trans. Instrum. Meas.*, vol. 44, no. 2, pp. 284–287, Apr. 1995.
[14] *IEEE Standard for Digitizing Waveform Recorders*, IEEE Std. 1057-1994, 1994.
[15] G. N. Stenbakken and J. P. Deyst, "Timebase nonlinearity determination using iterated sine-fit analysis," *IEEE Trans. Instrum. Meas.*, vol. 47, no. 5, pp. 1056–1061, Oct. 1998.
[16] C. M. Wang, P. D. Hale, and K. J. Coakley, "Least-squares estimation of timebase distortion of sampling oscilloscopes," *IEEE Trans. Instrum. Meas.*, vol. 48, no. 6, pp. 1324–1332, Dec. 1999.
[17] G. Vandersteen, Y. Rolain, and J. Schoukens, "An identification technique for data acquisition characterization in the presence of nonlinear distortions and timebase distortions," *IEEE Trans. Instrum. Meas.*, vol. 50, no. 5, pp. 1355–1363, Oct. 2001.
[18] C. M. Wang, P. D. Hale, K. J. Coakley, and T. S. Clement, "Uncertainty of oscilloscope timebase distortion estimate," *IEEE Trans. Instrum. Meas.*, vol. 51, no. 1, pp. 53–58, Feb. 2002.
[19] J. Verspecht, "Calibration of a measurement system for high frequency nonlinear devices," Ph.D. dissertation, Free Univ. Brussels, Brussels, Belgium, Sep. 1995.
[20] W. A. Fuller, *Measurement Error Models*. New York: Wiley, 1987.
[21] P. T. Boggs, R. H. Byrd, J. E. Rogers, and R. B. Schnabel, "User's reference guide for ODRPACK version 2.01 software for weighted orthogonal distance regression," U.S. Government Printing Office, Washington, DC, Nat. Inst. Stand. Technol. Internal Report, NISTIR 92-4834, Jun. 1992. [Online]. Available: http://www.boulder.nist.gov/mcsd/Staff/JRogers/odrpack.html
[22] *ODRPACK*. [Online]. Available: http://www.netlib.org/netlib/odrpack/
[23] P. T. Boggs, R. H. Byrd, and R. B. Schnabel, "A stable and efficient algorithm for nonlinear orthogonal distance regression," *SIAM J. Sci. Statist. Comput.*, vol. 8, no. 6, pp. 1052–1078, Nov. 1987.
[24] K. J. Coakley and P. Hale, "Alignment of noisy signals," *IEEE Trans. Instrum. Meas.*, vol. 50, no. 1, pp. 141–149, Feb. 2001.

Paul D. Hale (M'01–SM'01) received the Ph.D. degree in applied physics from Colorado School of Mines, Golden, in 1989.

He has been with the Optoelectronics Division, National Institute of Standards and Technology (NIST), Boulder, CO, since 1989 and has conducted research in birefringent devices, mode-locked fiber lasers, fiber chromatic dispersion, broadband lasers, interferometry, polarization standards, and high-speed optoelectronic measurements. He is presently the Leader of the High-Speed Measurements Project in the Sources and Detectors Group. His research interests include high-speed optoelectronic and microwave measurements and their calibration.

Dr. Hale is currently an Associate Editor of the JOURNAL OF LIGHTWAVE TECHNOLOGY. He has received the Department of Commerce Bronze, Silver, and Gold awards, two ARFTG Best Paper Awards, and the NIST Electrical Engineering Laboratory's Outstanding Paper Award.

C. M. Wang received the Ph.D. degree in statistics from Colorado State University, Fort Collins, in 1978.

He is a Mathematical Statistician with the Statistical Engineering Division, National Institute of Standards and Technology, Boulder, CO. His research interests include statistical metrology and the application of statistical methods to physical sciences.

Dr. Wang is a Fellow of the American Statistical Association.

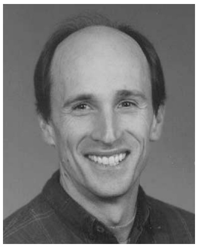

Dylan F. Williams (M'80–SM'90–F'02) received the Ph.D. degree in electrical engineering from the University of California, Berkeley, in 1986.

In 1989, he joined the Electromagnetic Fields Division, National Institute of Standards and Technology, Boulder, CO, where he develops metrology for the characterization of monolithic microwave integrated circuits and electronic interconnects. He has published more than 80 technical papers.

Dr. Williams is currently the Editor of the IEEE TRANSACTIONS ON MICROWAVE THEORY AND TECHNIQUES. He was the recipient of the Department of Commerce Bronze and Silver Medals, two Electrical Engineering Laboratory's Outstanding Paper Awards, two Automatic RF Techniques Group (ARFTG) Best Paper Awards, the ARFTG Automated Measurements Technology Award, and the IEEE Morris E. Leeds Award.

Kate A. Remley (S'92–M'99–SM'06) was born in Ann Arbor, MI, in 1959. She received the Ph.D. degree in electrical and computer engineering from Oregon State University, Corvallis, in 1999.

From 1983 to 1992, she was a Broadcast Engineer in Eugene, OR. From 1989 to 1991, she was the Chief Engineer of an AM/FM broadcast station. In 1999, she joined the Radio-Frequency Technology Division (now the Electromagnetics Division), National Institute of Standards and Technology, Boulder, CO, as an Electronics Engineer. Her research activities include metrology for wireless systems, characterizing the link between nonlinear circuits and system performance, and developing methods for improved radio communications for the public safety community.

Dr. Remley was the recipient of the Department of Commerce Silver Medal and the Automatic RF Techniques Group (ARFTG) Best Paper Award.

Joshua D. Wepman was born in Boulder, CO, where he attends Boulder High School.

He has been writing computer software for the National Institute of Standards and Technology, Boulder, since 2003.